GT2018-75432

MECHANICAL PROPERTIES IN GTD-111 ALLOY IN HEAVY FRAME GAS TURBINES

John R Scheibel
Electric Power Research Institute
Palo Alto, California, USA

Rajeev Aluru
Duke Energy
Raleigh, North Carolina, USA

Hans Van Esch
Turbine End User Services
Houston, Texas, USA

ABSTRACT

Nickel-based superalloys are extensively used in manufacturing hot gas path components in industrial gas turbines used for power generation. Specifically, GTD-111DS is one of the widely used alloys used in manufacturing the hot gas path rotating components. These components are subjected to extreme operating environments resulting in creep, oxidation, fatigue of the components during operation. After continued operation, these damage modes need to be repaired and the components go through extensive repair processes, which includes several heat treatments to recover the mechanical properties of the base material (GTD-111DS) lost during operation. The heat treatments used during repair by the different repair vendors can vary a lot in terms of temperature, time and the sequence as well. This study focuses on the understanding the difference in the effects of the heat treatments to the base material (partial solution, full solution, HIP and full solution) in terms of microstructure-mechanical property relationships. Results indicate that HIP and full solution resulted in refined microstructures and improved mechanical properties compared to the heat treatments involving partial solution or full solution only. Microstructure-mechanical property relationships suggest that components that need to be repaired beyond OEM recommended repair intervals benefit from the HIP and full solution heat treatments.

KEY WORDS

GTD 111DS, Combustion turbine, Hot isostatic pressing, Repair, Solution heat treatment, Mechanical properties

INTRODUCTION

Combustion turbines (CT) have become an increasingly important segment of power generation portfolio globally because of their relatively high efficiency, reduced emissions and abundant supply of natural gas. Due to the high firing temperatures and consumable component design philosophy employed by combustion turbine technologies, the associated maintenance cost for CT fleet typically reaches several million dollars. These costs are related primarily to the replacement and repair of hot section parts used in the turbine engines. Hence, understanding component design life including the design intent, details of the repairs performed during its life time, and improvement of the mechanical properties during the repair is very crucial for managing the reliability and maintenance costs of the combustion turbines. The overall approach used for component life extension study performed is described elsewhere [1,2]. The component life extension includes a methodical approach including a deeper understanding of the degradation of the base material microstructure-mechanical property relationships with service, and the improvement of properties with repairs.

One of the widely used alloys for manufacturing combustion turbine rotating components is GTD-111 DS. The repair of the components made out of GTD-111DS involves several heat treatments to bring the desired mechanical properties to the base material, that were lost during operation. Some of the heat treatments performed during repair consists of 2050F for 2-4 hours at several stages of the process (Partial Solution), HIP (Hot Isostatic Pressing) at (2150F-2200F)/2 hrs, and full solution (2150F-2200F)/2 hrs, as required by the repair vendors processes and specifications. There is no common standard or agreement as far as the sequence or the heat treatment protocol followed during repair. On the other hand, EPRI F7FA S1B repair specifications (which was developed by TEServices) recommends full and partial solution heat treatments followed by aging cycle. The requirement of HIP prior to full solution heat treatment is based on metallurgical evaluation, operation and repair history of the buckets or customer preference. But, no further guidance on the microstructural criteria that dictates the full solution and HIP was provided. Hence, the turbine owner primarily relies on repair vendors for the heat treatments to be performed.

The criteria to be used during the heat treatment selection should be based on the required mechanical properties, required microstructure, optimizing the microstructure-mechanical property relationships and the cost incurred during the repairs

because of the heat treatments. Several authors studied the heat treatments and resulting microstructures from those heat treatments and concluded that the high temperature solution treatment is beneficial for improved microstructure [3,4,5]. However, the mechanical properties resulting from the heat treatments and the deterioration of the properties of the buckets with service, and the relationship between the microstructure-mechanical properties are unavailable to understand the full impact of the heat treatments and thereby make a final decision on repairability. Hence, this study is focused on understanding the effect of different heat treatments in terms of microstructure and mechanical properties on GTD-111 alloy in different service conditions from the serviced buckets.

SPECIMENS AND TEST CONDITIONS:

The nominal composition of GTD-111DS alloy is given in the table below [6].

Element	Ni	Cr	Co	Mo	Ti	Al	C	W	Ta	Cb	B
wt%	Bal	13.6	9.14	1.6	4.9	2.97	0.090	3.440	2.870	<0.01	0.010

Table 1: Nominal Composition of GTD-111 DS Alloy

CONDITION OF THE BUCKETS USED:

Combustion turbine operating intervals vary according to starts or hours based intervals. Typically, turbine blades or buckets will be operated for 800-900 starts (1 interval-starts) and /or 24,000 hours (1 interval-hours) before they were disassembled from the machine and sent to the repair. After successful completion of the repair, the components will be assembled into the turbine and will be operated for another service interval as mentioned above. At that point, the parts would have accumulated 1600-1800 starts (2 intervals-starts) and/or 48,000 hours (2 intervals-hours). For the current study, we will be referring to the 1 interval and 2 intervals components in the as-received and repaired condition.

This study included a total of forty two service run stage 1 buckets, at varying conditions including 1 interval-as run, 2 intervals-as run, 2 intervals repaired-partial solution, 2 intervals repair-HIP plus full solution, 2 intervals repair-full solution. (The buckets that accumulated two intervals were repaired after their first interval possibly with a partial solution heat treatment, however the exact heat treatments used during 1st repair were unknown) In addition, the buckets appear to be cast from two different suppliers, which included a prefix C2NM or C2NP, that showed some differences in design attributes that resulted in varying scrap rates. Hence, the investigations focused on the two styles M and P to understand the differences in properties. The testing performed on as-run buckets was intended to quantify service degradation, and the testing performed on repaired buckets was intended to quantify the improvement obtained with heat treatments.

HEAT TREATMENTS INVESTIGATED:

Heat Treatment-1	Heat Treatment-2	Heat Treatment-3
Pre-weld HT 2050°F for 4 hours	Pre-weld HT 2050°F for 4 hours with slow or fast cool	HIP at 2190°F ±25°F for 4 hours with minimum 15K PSI in Argon
Post-weld HT 2050°F for 2 hours	Post-weld HT 2150°F for 2 hours	Full solution at 2175°F ±25°F for 2 hours in vacuum and argon quenched
Diffusion- MCrAlY coating 2050°F for 2 hours	Diffusion- HVOF coating 2050°F for 2 hours	partial solution and age at 2050°F ±25°F for 2 hours (controlled cooling)
Diffuse TBC coating 2050°F for 2 hours	Diffusion- TBC coating 2050°F for 2 hours	Diffusion- HVOF coating 2050°F for 2 hours
age 1550°F for 24 hours all in vacuum	age 1550°F for 24 hours all in vacuum	Diffuse TBC coating HT 2050°F for 2 hours
		1550°F for 24 hours and argon quenched both in vacuum.

Table 2: Heat Treatments used for the Study

SECTIONING PLAN AND MECHANICAL TESTING DETAILS:

The sectioning plan for microstructural investigations included five sections taken across the length of the blade as shown in Figure 1. The details of the sections are provided in the Table 3. The root section is used for comparison of microstructure from the new manufacture, as this area is not exposed to higher temperatures. Microstructural investigations included low magnification optical microscopy to determine porosity levels, carbide structures and high magnification scanning electron microscopy to study and compare the gamma-prime morphology.

Metallurgical Section Location	**Dimension (from tip of the blade)**	**Notation**
Trailing Edge (TE)-Tip	0.25 inch (0.635 cm)	TE
Leading Edge (LE) Tip	1 inch (approximately 2.54 cm)	LE
Mid airfoil Longitudinal	4 inches (approximately 10.16 cm)	ML
Mid airfoil Transverse	4 inches (approximately 10.16 cm)	MC
Root Tab	Root	RT

Table 3: Details of Sections Taken for each Blade

Mechanical property testing of the buckets focused on two locations- airfoil and platform, primarily on stress rupture properties and low cycle fatigue (LCF) properties. Mechanical testing included stress rupture testing at 1600°F/40 Ksi and low cycle fatigue testing at 1650°F, 0.7% strain range. The specimens for mechanical testing are detailed in Figure 2. The stress rupture tests included two cylindrical stress rupture specimens from airfoil in the longitudinal direction, and one flat specimen from platform in the transverse direction, and the LCF tests included one cylindrical specimen from the airfoil in the longitudinal direction and another cylindrical specimen from the platform in the transverse direction. The locations of the specimens were obtained from the finite element models generated as a result of the studies published elsewhere [1].

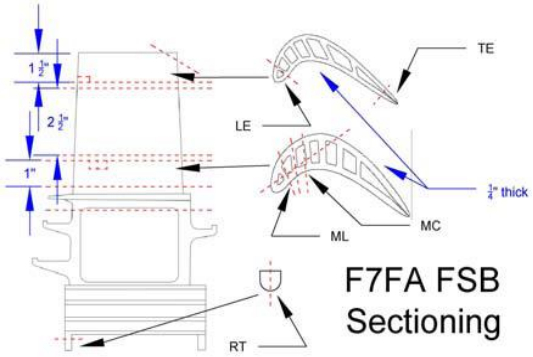

Figure 1: Sectioning Plan used for the Study

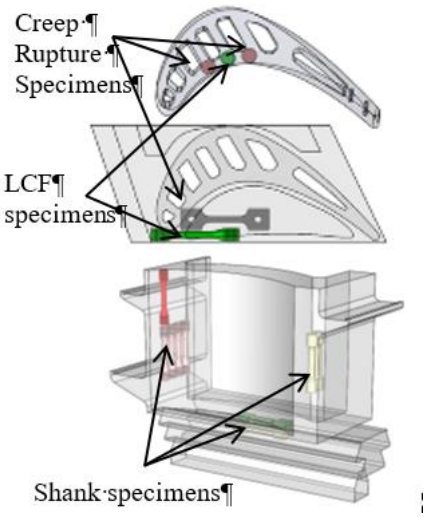

Figure 2: Mechanical Testing Specimen Plan used for the Study

RESULTS:

MICROSTRUCTURAL INVESTIGATIONS:

One interval buckets: (318 - 899 starts and 5,243 - 7,298 hours) [As-Run condition]

Un-etched metallurgical evaluation using optical microscope in the As-Run (AR) condition showed some casting porosity in all buckets in all locations including the root. The carbide distribution was relatively small and nicely defined with a little larger carbide concentration of the P buckets compared to the M buckets. [As explained before, M and P indicated two different casting vendors.] Etched metallurgical evaluation using optical microscope showed minor differences in the dendrite and grain size all buckets. Also, linear secondary phases were present in these sections. These linear phases were determined to be rich in heavy elements such as tantalum, tungsten, and chromium. These phases will be discussed in detail later at the end of the current section. In most cases, casting porosity and inclusions also accompanied these linear phases and the concern was that these linear phases and imperfections possibly influence the stress rupture and Low Cycle Fatigue (LCF) properties.

Scanning electron microscopy of the same sections was performed to study the gamma-prime morphology and distribution. Figure 3 provides representative detail on the inter-dendritic (outside the dendirite arm) and intra-dendritic (inside the dendrite) regions for reference. Figure 4 represents the microstructure of the bucket in as-run condition. The morphology appears to be different between inter-dendritic and intra-dendritic regions. The primary gamma prime of the inter-dendritic regions appear to be smaller and more cuboidal of shape than intra-dendritic regions. The size of gamma-prime was compared across different regions and the root section was assumed to be the baseline. The primary gamma prime at the TE was rounded and grown significantly (1.0 - 1.8 μm, spherical), and the growth was somewhat less significant at the LE (0.7 - 1.2 μm, spherical / rounded). At the mid airfoil cross and longitudinal sections, the size of the primary gamma prime (0.7 - 1.0 μm, rounded) was just a little larger than the root (0.6 - 1.0 μm, rounded /cuboidal) and maintained almost the same shape compared to the root. The secondary gamma prime was mostly not present at the TE, less present at the LE and about the same size (0.10 - 0.20 μm) and shape (spherical) at the mid airfoil and root.

Two intervals buckets-starts based: 1,650 starts and 12,372 hours [As-run condition]

As mentioned above, the buckets that accumulated two service intervals underwent a repair after their first interval and the details of that repair are unknown. Metallurgical evaluation of the 2 intervals buckets in as-run condition showed similar microstructure as the one interval buckets except that the larger sized carbides and higher concentration of carbides were present in 2 intervals buckets compared to 1 interval buckets. The linear secondary phases associated with casting imperfections were also similar to the ones see in one-interval buckets.

Scanning electron microscopy revealed that the primary gamma prime of the inter-dendritic regions was smaller and more cuboidal of shape than the intra-dendritic regions, similar to the one interval buckets. Figure 4 represents the microstructure of the bucket in as-run condition. The primary gamma prime had rounded in shape and grown significantly at the TE (1.2 – 1.8 μm - spherical) and somewhat grown less significantly at the LE (0.8 – 1.2 μm – rounded). At the mid airfoil, the primary gamma prime size (0.8 – 1.0 μm –rounded), was just a little larger than at the root (0.8 – 0.9 μm rounded) and maintained the same shape compared to the root. It needs to be noted that the relatively large size and rounded shape of the primary gamma prime at the root indicates that these buckets possibly did not receive the optimum HT's during the new manufacture or at the first repair. The secondary gamma prime was nearly not present at the TE and about the same size (0.10 - 0.20 μm) and shape (spherical) at the LE, mid airfoil and root. It needs to be noted that the volume fraction of secondary gamma prime at LE increased when compared to the first cycle buckets.

Microstructural investigations on one-interval and two-intervals buckets revealed that the size of the primary gamma-prime increased significantly in the LE and TE areas of the buckets (hottest regions of the bucket), compared to the root section.

Two intervals buckets-one hours based and one starts based: 1,100-1200 total starts and 24,000-36,000 total hours [As-run condition].

This section refers to the evaluation of the group of buckets that accumulated two service intervals with a repair after its first cycle. The heat treatment details of that repair are unknown. The metallurgical structure of the base material (carbide and gamma prime structure) have coarsened, grain boundaries are sensitized by the presence of elongated carbides and some needlelike (carbide) phases with gamma prime eutectics were observed. It appears that the metallurgical condition (carbide and gamma prime structure) has aged during operation. The primary gamma prime grown significantly at the TE (1.4 – 1.9 μm - spherical) and somewhat grown less significantly at the LE (0.6 – 0.8 μm – rounded), compared to the one interval buckets. Figure 5 represents the microstructure of the buckets that accumulated two intervals in the as-run condition.

In summary, for the as-run buckets in different conditions, microstructural investigations on one-interval and two-intervals buckets revealed that the size of the primary gamma-prime increased significantly in the TE area (hottest regions of the bucket), and less significantly in the other areas of the buckets compared to the root section.

		1 Interval Buckets (318 - 899 starts and 5,243-7,298 hrs.)		2 Intervals Buckets-starts based (1,650 starts and 12,372 hours		2 Intervals Buckets-one hours based and one starts based (1,100-1200 starts and 24,000 hours)	
Location		**Primary Gamma Prime Size [µm]**	**Secondary Gamma Prime Size [µm]**	**Primary Gamma Prime Size [µm]**	**Secondary Gamma Prime Size [µm]**	**Primary Gamma Prime Size [µm]**	**Secondary Gamma Prime Size [µm]**
TE	Trailing Edge (TE)	1.0-1.8	N/A	1.2-1.3S	N/A	1.4-1.9 S	N/A
LE	Leading Edge (LE)	0.7-1.2	N/A	0.8-1.2 R	0.1-0.2	0.6-0.8 R	0.1
MC	Mid airfoil Cross section	0.7-0.9	0.15	0.9-1.0 R	0.1-0.2	0.7-0.9 R	0.1
ML	Mid airfoil Longitudinal section	0.7-0.8	0.15	0.8-0.9 R	0.1-0.2	0.8-1.0 R	0.10
RT	Root (RT)	0.6-0.9	0.15	0.8-0.9 R	0.15-0.2	0.6-0.8 R	0.05
Note: C – Cuboidal R – Rounded S - Spherical							

Table 4: Gamma-prime Size Evaluation for 1-interval and 2-intervals Buckets

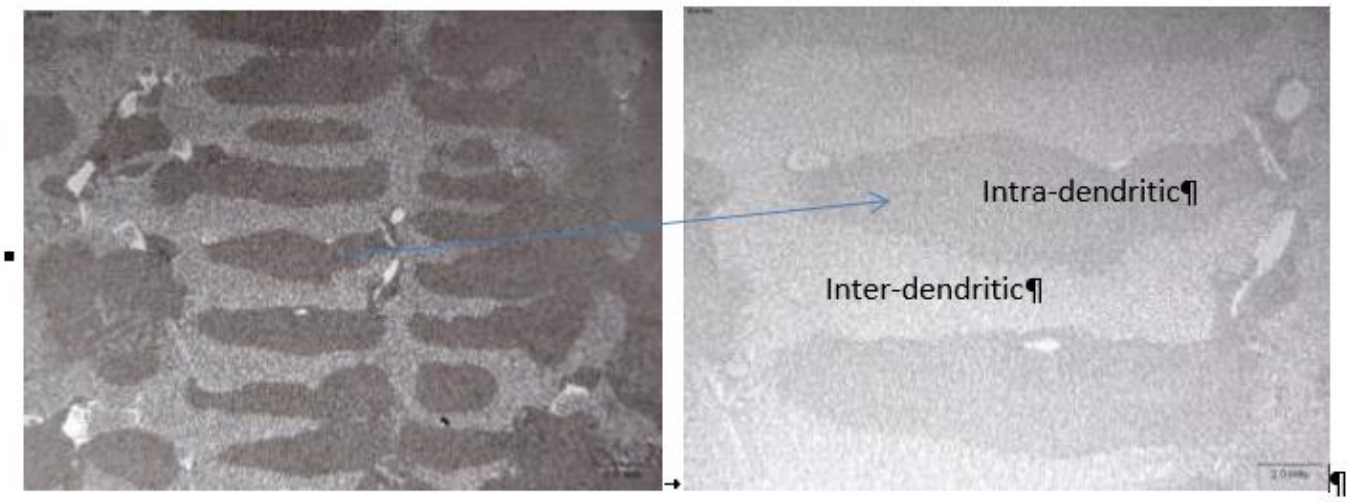

Figure 3: Representative Micrograph Showing Inter-dendritic and Intra-dendritic Regions.
The picture on left shows dendritic microstructure and the one on right shows more detail on the difference in gamma-prime.

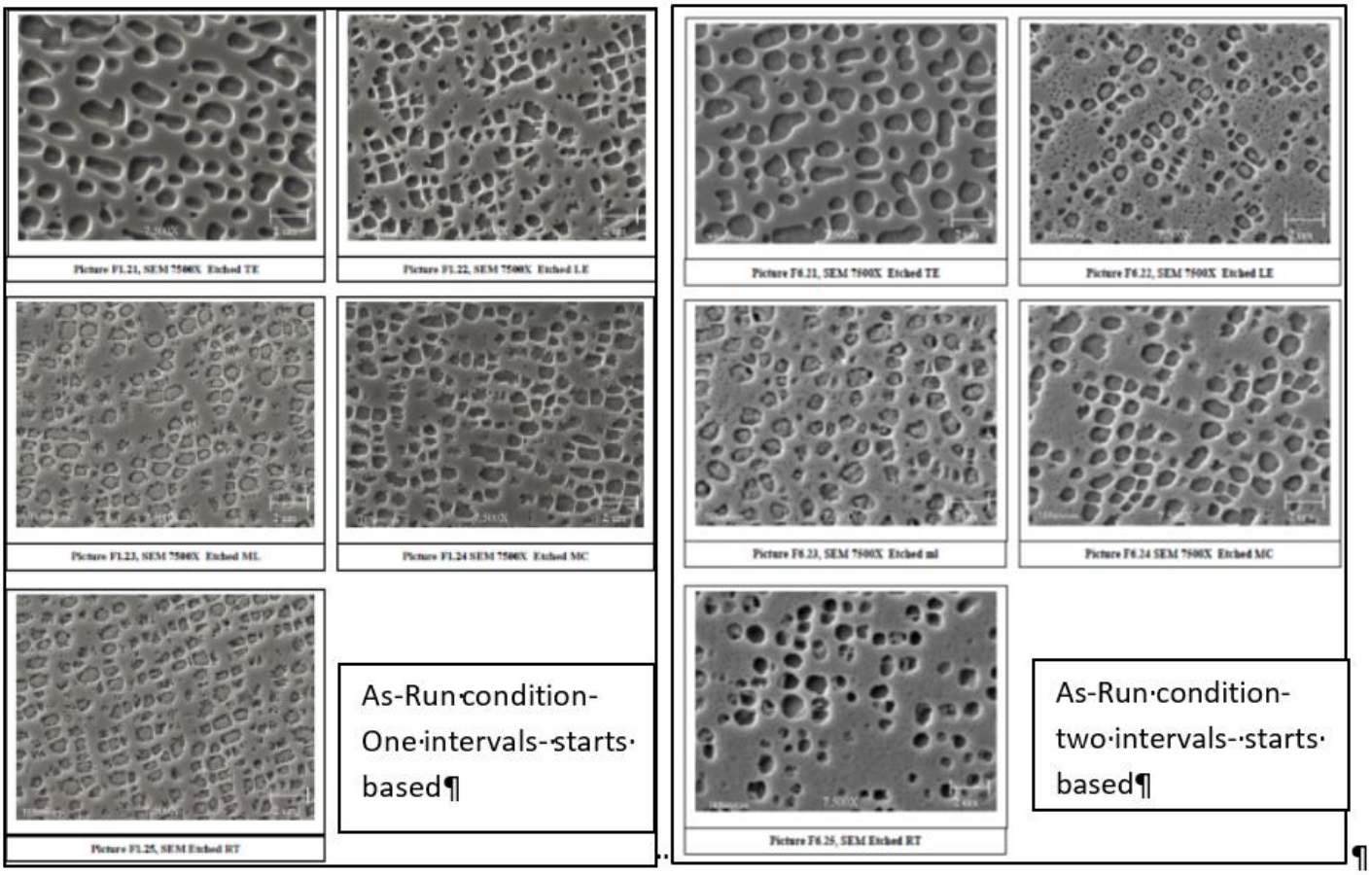

Figure 4: Microstructure of the Specimens Extracted from Buckets after One Interval-starts based (on the left) and Two Intervals-starts based in As-run Condition (on the right)

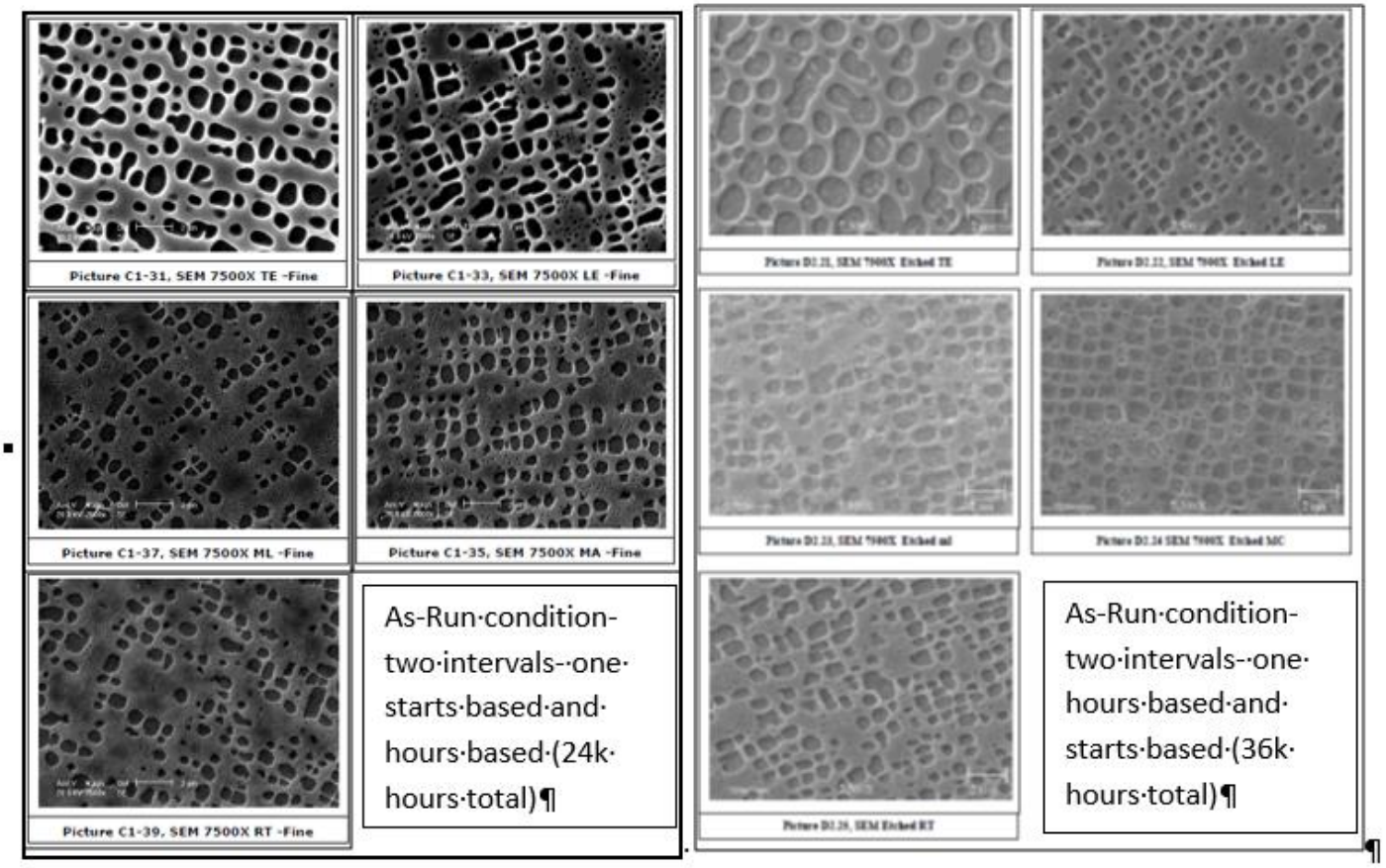

Figure 5: Microstructure of the Specimens Extracted from Buckets after Two Intervals-one starts based and one hours based in As-run Condition [buckets accumulated 24k total hours on the left and the ones accumulated 36k total hours on the right]

Two-intervals Buckets: 1,650 starts and 12,372 hours [Repaired condition].

Repaired buckets included buckets processed in three conditions listed in Table 2. Metallurgical evaluation of the buckets showed larger carbides distribution for the ones processed using heat treatments-1 compared to the buckets processed using other two heat treatments. This might be due to the partial solutioning of carbides in heat treatment-1 as opposed to full solutioning in other two heat treatments. On the other hand, the larger carbide size from heat treatment-1 appears to be similar to the unrepaired buckets. This indicates that heat treatment-1 resulted in almost unchanged carbide structure compared to as-run condition.

Scanning electron microscopy revealed significant differences of gamma-gamma prime morphology between different heat treatments. This can be seen in Figure 7 and Figure 7. Figure 7 represents the microstructure in buckets processed using heat treatment-1 and heat treatment-2, whereas Figure 7 represents the microstructure of the buckets processed using and heat treatment-3. It needs to be noted that the buckets from the same set were selected for as-received and different heat treatments so that accurate comparison of the microstructures with different heat treatments can be performed. Higher amounts of cuboidal primary gamma prime (0.4 – 0.5 µm) with some spherical shaped (0.10 – 0.15 µm) was observed in buckets processed using heat treatment-3 sequence. The size of gamma-prime in the non-dendritic and dendritic locations was observed to be in the range of (0.4 – 0.5 µm), and (0.8 – 1.0 µm) respectively. In contrast, in the buckets heat treated using sequence 1 and 2, large rounded primary gamma prime (0.8 - 1.2 µm) were observed.

Microstructural investigations on repaired two-intervals buckets revealed that heat treatment-3 resulted in better morphology including refined gamma-gamma prime distribution and higher volume fraction. The average gamma prime size in heat treatment-3 is in the order of 0.4-0.5 µm opposed to 0.8-1.0 µm in the case of other heat treatments. In addition, heat treatment-3 resulted in smaller secondary gamma-prime size and lower volume fraction compared to the other heat treatments. Hence, it appears that heat treatment-3

results in an optimized microstructure similar to better than the original condition. This size distribution and the possible impact of the microstructure on mechanical properties will be discussed in the next section.

		Heat Treatment-1		Heat Treatment-2		Heat Treatment-3	
Location		**Primary Gamma Prime Size [µm]**	**Secondary Gamma Prime Size [µm]**	**Primary Gamma Prime Size [µm]**	**Secondary Gamma Prime Size [µm]**	**Primary Gamma Prime Size [µm]**	**Secondary Gamma Prime Size [µm]**
TE	Trailing Edge	0.8 R	0.15	1.3R /0.4C	N/A	0.4 C / 0.8 R	Few 0.2
LE	Leading Edge	0.8 R	0.15	1.5 R/ 0.4 C	N/A	0.5 C / 1.0 R	Few 0.2
MC	Mid airfoil Cross section	1.2 R	0.15	0.9 R/ 0.5 C	0.15	0.4 C / 0.9 R	Few 0.2
ML	Mid airfoil Longitudinal section	1.2 R	0.15	1.0 R /0.5 C	0.15	0.5 C / 0.9 R	Few 0.2
RT	Root	1.4 S	0.15	1.0 C /0.4C	0.15	0.4 C / 0.8 R	Few 0.1
Note: C – Cuboidal R – Rounded S - Spherical							

Table 5: Gamma-prime Size for the Buckets Processed using Different Heat Treatments

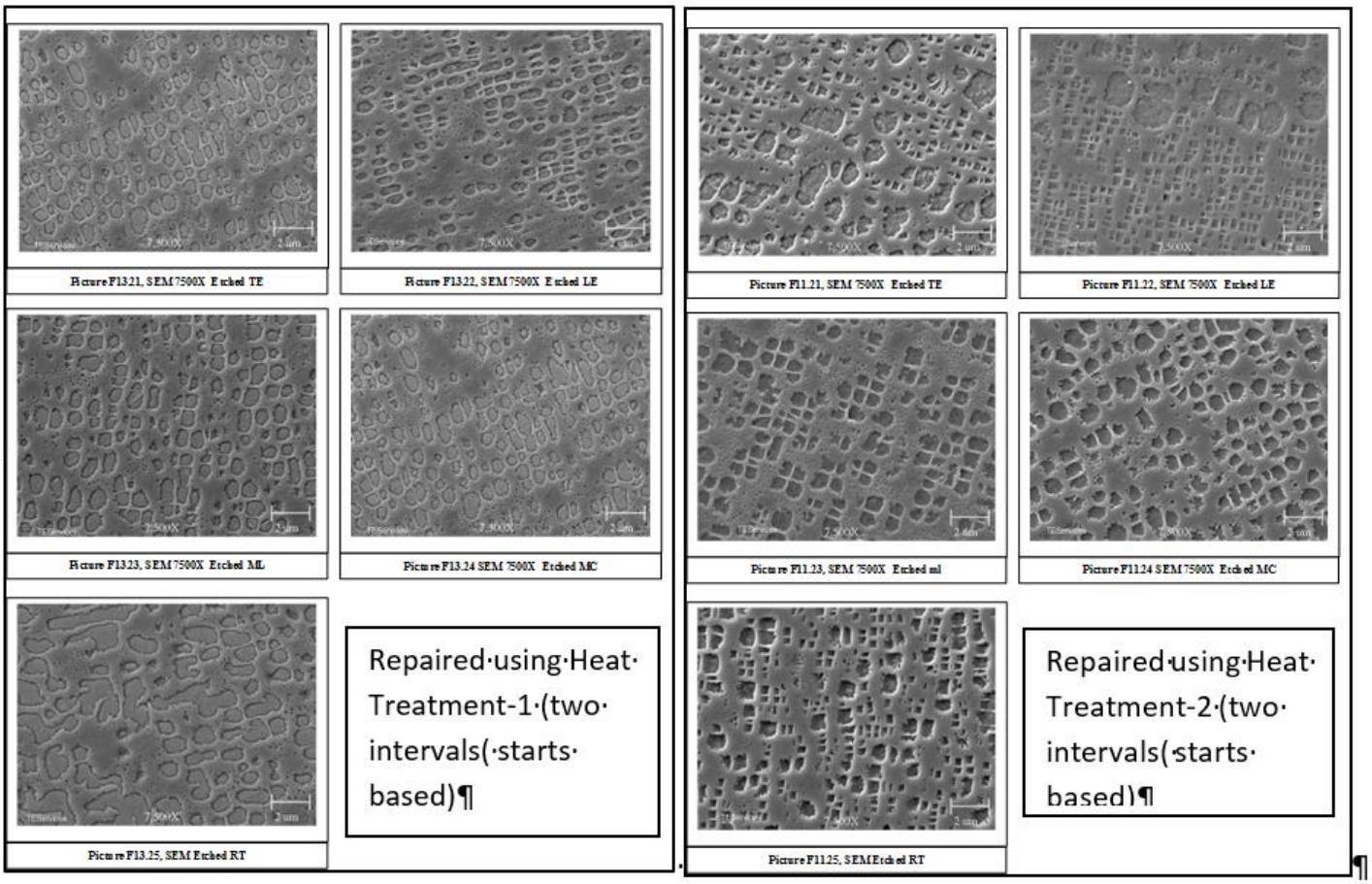

Figure 6: Microstructure of the specimens extracted from buckets after two starts based intervals and treated with heat treatment-1 (on the left) and heat treatment-2 sequence (on the right). [Details of the sequence were listed in Table 2.]

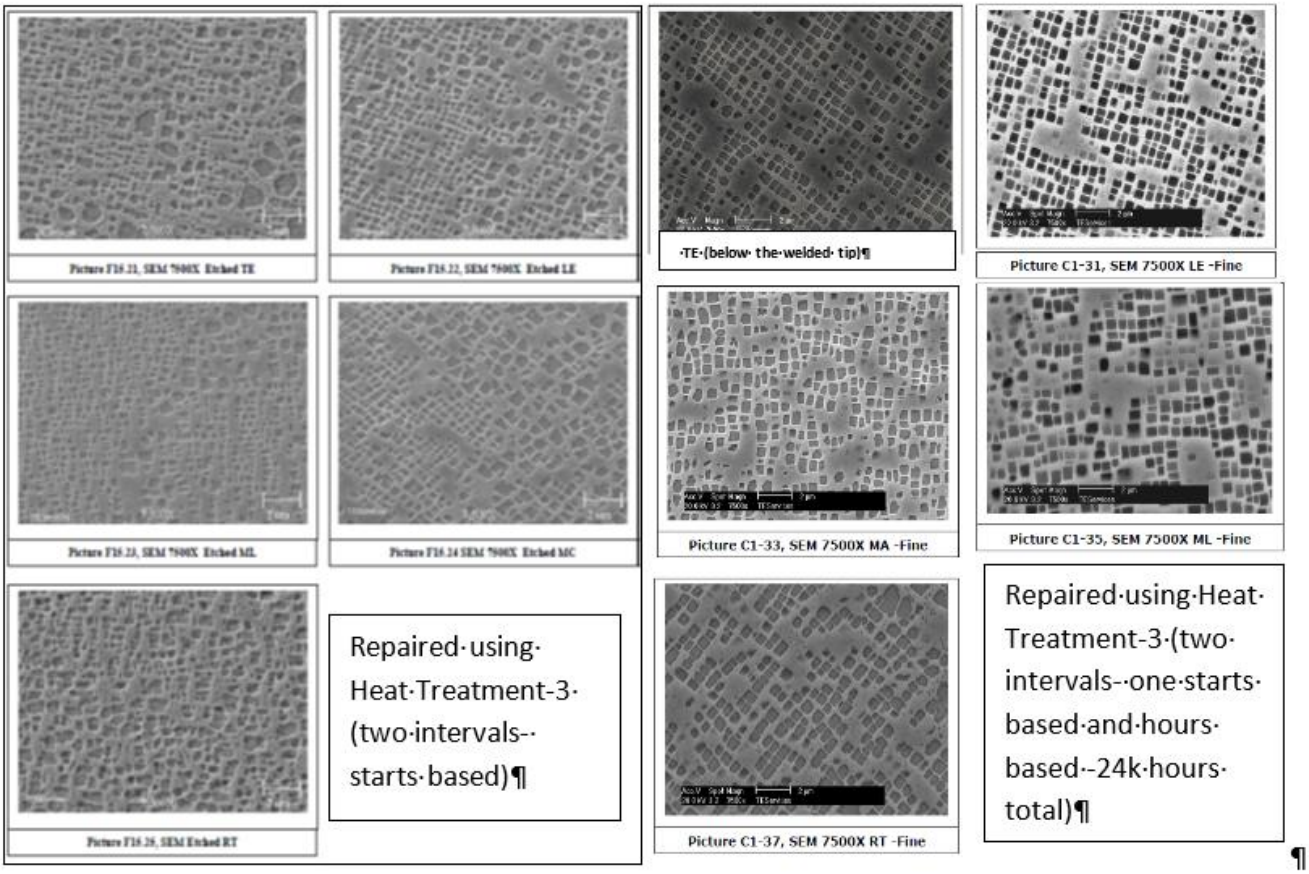

Figure 7
Microstructure of specimens extracted from buckets processed using heat treatment-2 and heat treatment-3 sequence. [Details of the sequence were listed in Table 2.]

LINEAR PHASES

As mentioned before, needle-like secondary phases observed during metallurgical evaluations were studied further. These secondary phases were also accompanied by casting defects such as inclusions. EDS analysis of the phases determined that these appear to be tantalum and titanium carbides (MC). The blocky "carbides" and other linear and X-hatched needlelike phases showed also C, Ta and Ti, however significant amount of Cr was also observed. Figure 8 represents the semi-quantitative EDS (Energy Dispersive Spectroscopy) analysis of these secondary phases.

Based on metallurgical evaluations of the 1-interval, 2-intervals and repaired buckets, these phases appear to be formed during casting and following heat treatments during the manufacturing process. It is possible that these phases grow a little during operation at the higher temperature locations (airfoil) and change (grow and reduce in size) during the repair heat treatments. These phases possibly reduce the mechanical strength of the base material during operation at that location, however it appears that the OEM has accepted the material condition and mechanical properties with these phases.

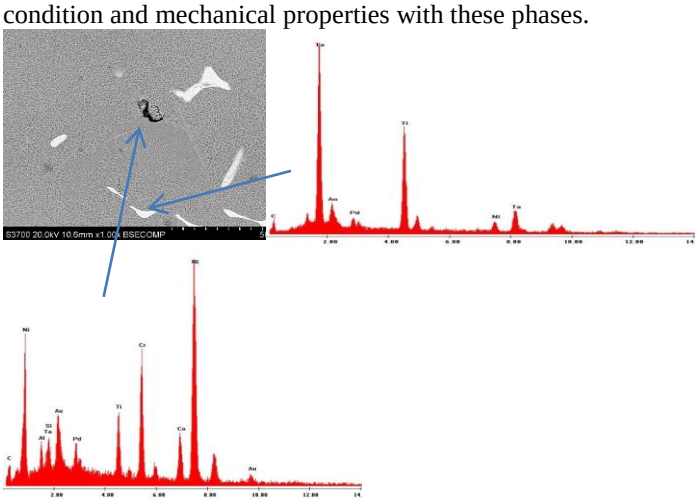

Figure 8: EDS of Needle-like Secondary Phases Observed in the Microstructure

MECHANICAL PROPERTIES

Stress Rupture: Figure 9 represents the average of stress rupture properties of airfoil specimens extracted from buckets, after accumulating 6000 (6k), 12,000 (12k), 24,000 (24k) hours of service. The buckets exposed to 12k, 24k hours have been through two service intervals which includes a repair after one service interval. One recommended service interval for the buckets equals 800 starts or 24,000 hours for a starts based operation (simple cycle) and hours based operation (combined cycle) respectively.

It appears that the stress rupture properties of the airfoil at 12k, 24k decreased with time when compared to 6k hours, due to exposure to operating temperatures for higher times as expected. On the other hand, the stress rupture properties increased significantly after repairs that involved any of the heat treatment. However, the improvement in properties resulted from heat treatment-1 and 2 (listed as repaired-partial solution treatment) were inferior compared to the properties resulted from heat treatment-3 (listed as repaired-full solution). The increase in properties can be attributed to the more refined microstructure including increased volume fraction of gamma-gamma prime as explained in the previous sections.

Figure 10 represents the average of stress rupture properties of platform specimens extracted from buckets, after accumulating 6000 (6k), 12,000 (12k), 24,000 (24k) hours of service. Stress rupture properties of flat specimens extracted from platform in the transverse direction revealed similar improvements from repair as the airfoil specimens. However, the improvement in properties of platform was much higher in scale for the platform specimens compared to the airfoil specimens. This can be possibly explained due to the microstructural improvements contributing more to the transverse direction than the directionally solidified airfoil. Also, the average of the platform specimens that accumulated 24k hours in the as-run condition measured higher than the average of specimens accumulated 12k hours. This can be explained based on the standard deviation in the samples and the scatter associated with the test results.

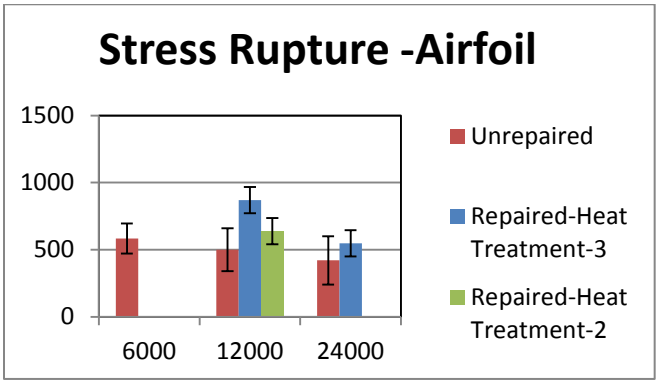

Figure 9: Average values of stress rupture properties of specimens extracted from airfoil (Error bars represent one standard deviation)

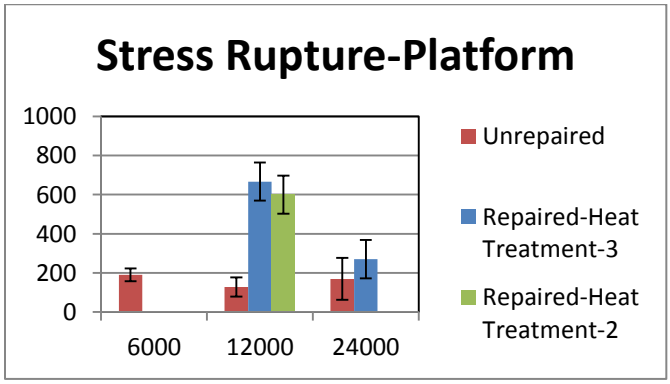

Figure 10: Average values of stress rupture properties of specimens extracted from platform (Error bars represent one standard deviation)

LOW CYCLE FATIGUE PROPERTIES

Figure 11 represents the average cycles to failure for LCF specimens extracted from the platform of the buckets, after accumulating 800 and 1200 starts in service. The buckets exposed to 1200 starts have been through two service intervals which includes a repair after one service interval. As mentioned above, one recommended service interval for the buckets equals 800 starts or 24,000 hours for a starts based operation (simple cycle) and hours based operation (combined cycle) respectively. As expected, LCF properties (cycles to failure) of the platform specimens at 1200 starts decreased with time when compared to 800 starts, due to accumulation of fatigue during each and every stop.

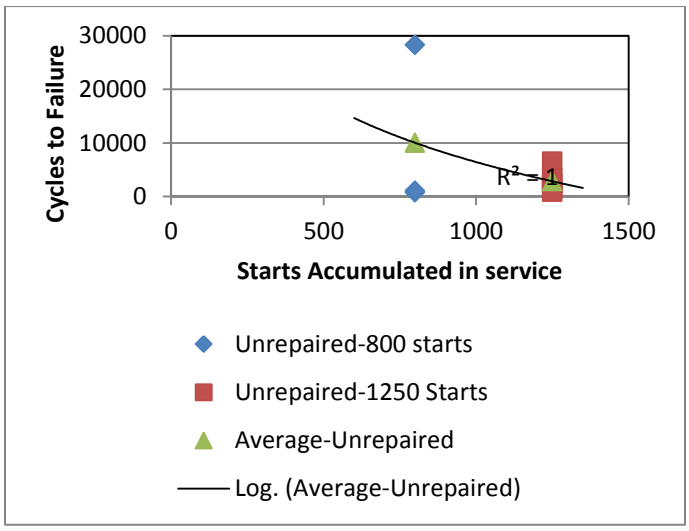

Figure 11: LCF Life of Specimens Extracted from Platform

Figure 12 represents the average of cycles to failure for platform specimens extracted from buckets, after accumulating 800, 1200, and 1600 starts in service in unrepaired and repaired conditions. From the chart, it appears that the specimens from buckets that accumulated 1600 starts exhibited higher average LCF life in as-run condition compared to the specimens from buckets accumulated 800 starts. This might be due to the scatter associated with the fatigue testing and it can be also seen in the range of the obtained values provided in the graph. In addition, the LCF properties increased significantly after repairs. The repairs performed on the buckets involved the heat treatment-3 as listed in Table 2, which included HIP and full solution. This might be related to the refined microstructure observed in the samples with that heat treatment.

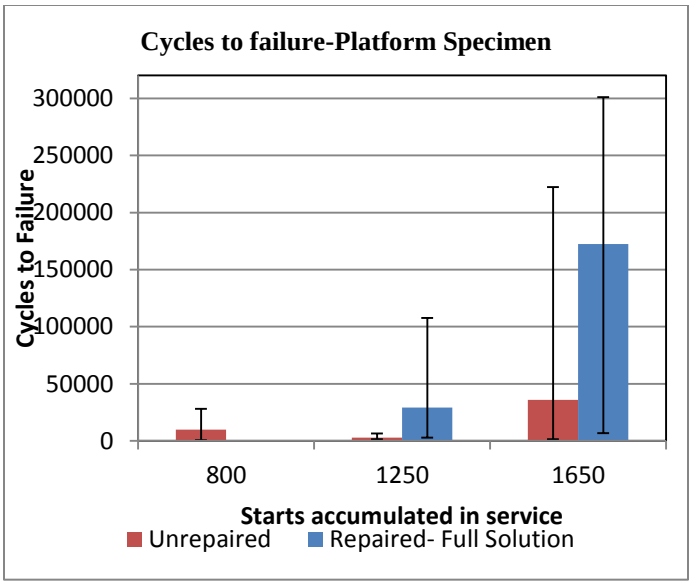

Figure 12: Average LCF life of specimens extracted from platform [Error bars represent the range of results obtained-lowest and highest values obtained in the tests]

CONCLUSIONS:

Microstructure-mechanical property relationships for several service conditions and various heat treatments were investigated. Service run buckets showed significant microstructural degradation in the trailing edge area compared to the other areas of the bucket. Repairs involving any heat treatment showed improvements in microstructure-mechanical properties. However, Heat treatment-3 involving HIP followed by full solution resulted in improved microstructure and mechanical properties compared to other heat treatments that involve partial solution only, and the ones without HIP. Buckets that accumulated two intervals with extended hours and starts showed significant degradation in microstructure and mechanical properties, however the full solution treatments resulted in improvement of properties. In addition, platform appears to be degrading more than the airfoil in terms of creep and LCF. It can be reinstated that platform appears to the weak link based on the reduction in the properties.

Although the higher temperature solution treatment appears to be better in terms of microstructure and mechanical property relationships, further secondary effects of the same in terms of recrystallization effects, diffusion of internal aluminide coating, integrity of braze ball present in the internal serpentine cooling passage needs to be studied. These effects are being investigated.

REFERENCES

[1] E. Wan, P. Crimi, J. Scheibel, R. Viswanathan, Proceedings of ASME TURBO EXPO 2002, Amsterdam, June 2002
[2] J. Scheibel, R.Aluru, H. Van Esch, R. Dewey, Proceedings of ASME TURBO EXPO 2012, Copenhagen, June 2012.
[3] S.A. Sajjadi, S. Nategh, R.I. Guthrie, Materials Science and Engineering A, 2002, 325,Pages 484-489.
[4] Hyung-Ick Kim, Hong-Sun Park, Jae-Mean Koo and Chang-Sung Seok, Sung-Ho Yang and Moon-Young Kim,
J. Mech. Sci and Technol., 26 (7), (2012), 2019-2022
[5] P. Wangyao, / V. Krongtong, / N. Panich, / N. Chuankrerkkul, / G. Lothongkum, High Temperature Materials and Processes. Volume 26, Issue 2, Pages 151–160, May 2011.
[6] R. Viswanathan, Gas turbine blade superalloy material property handbook (TR 1004652, EPRI, 2001).